Accepted Manuscript

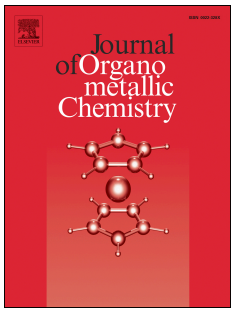

Synthesis, X–ray Structures, Spectroscopic Analysis and Anticancer Activity of Novel Gold(I) Carbene Complexes

Muhammad Altaf , M. Monim–ul–Mehboob , Adam A.A. Seliman , Anvarhusein A. Isab , Vikram Dhuna , Gaurav Bhatia , Kshitija Dhuna

PII: S0022-328X(14)00211-3

DOI: 10.1016/j.jorganchem.2014.04.029

Reference: JOM 18564

To appear in: *Journal of Organometallic Chemistry*

Received Date: 10 March 2014

Revised Date: 28 April 2014

Accepted Date: 28 April 2014

Please cite this article as: M. Altaf, M. Monim–ul–Mehboob, A.A.A. Seliman, A.A. Isab, V. Dhuna, G. Bhatia, K. Dhuna, Synthesis, X–ray Structures, Spectroscopic Analysis and Anticancer Activity of Novel Gold(I) Carbene Complexes, *Journal of Organometallic Chemistry* (2014), doi: 10.1016/j.jorganchem.2014.04.029.

Synopsis

This paper report the three new linear gold(I) complexes of the formulae [Au(Ipr)($S_2CN(CH_3)_2$)] (**1**), [Au(Ipr)($S_2CN(C_2H_5)_2$)] (**2**) and [Au(Ipr)($S_2CN(C_7H_7)_2$)] (**3**) [where Ipr = 1,3-Bis(2,6-di-isopropylphenyl)imidazol-2-ylidenegold]. These complexes have been prepared by the reaction of equimolar amounts of 1,3-Bis(2,6-di-isopropylphenyl)imidazol-2-ylidenegold(I)chloride, [Au(Ipr)(Cl)] with sodium dimethyldithiocarbamate monohydrate, sodium diethyl dithiocarbamate trihydrate and dibenzyl dithiocarbamate respectively. The cytotoxic evaluations against A549, HCT15 and HeLa human cancer lines are reported.

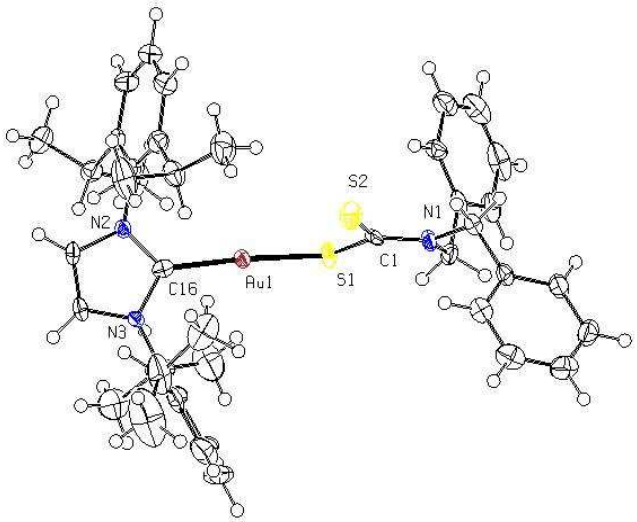

Synthesis, X–ray Structures, Spectroscopic Analysis and Anticancer Activity of Novel Gold(I) Carbene Complexes

Muhammad Altaf[a], M. Monim–ul–Mehboob[a], Adam A. A. Seliman[a], Anvarhusein A. Isab[a,*], Vikram Dhuna[b], Gaurav Bhatia[b], Kshitija Dhuna[c]

[a]*Department of Chemistry, King Fahd University of Petroleum and Minerals, Dhahran–31261,Saudi Arabia*
[b]*Department of Biotechnology, DAV College, Amritsar–143001, Punjab, India*
[c]*Department of Molecular Biology and Biochemistry, Guru Nanak Dev University, Amritsar–143005, Punjab, India*

*Corresponding author. Tel.: +966-13860-2645
E–mail address: aisab@kfupm.edu.sa (Anvarhusein A. Isab).

Abstract

Three new linear gold(I) complexes of the formulae [(Ipr)Au($S_2CN(CH_3)_2$)] (**1**), [(Ipr)Au ($S_2CN(C_2H_5)_2$)] (**2**) and [(Ipr)Au($S_2CN(C_7H_7)_2$)] (**3**) [where Ipr = 1,3–Bis(2,6–di–isopropylphenyl)imidazol–2–ylidenegold] have been prepared by the reaction of equimolar amounts of 1,3–Bis(2,6–di–isopropylphenyl)imidazol–2–ylidenegold(I)chloride, [(Ipr)Au(Cl)] with sodium dimethyldithiocarbamate monohydrate, sodium diethyl dithiocarbamatetrihydrate and dibenzyldithiocarbamate, respectively. The structures of the complexes have been determined by single X–ray crystallography. All gold(I) complexes (**1**–**3)** are iso–structural i.e. linear geometry. The complex (**1)** crystallizes in monoclinic space group 'P 2_1/a', while the complexes (**2)** and **(3)** crystallize in orthorhombic space group 'P na2_1'. The IR spectra and ^{1}H as well as ^{13}C NMR measurements of the Au(I) complexes (**1**–**3)** corroborate well with their single crystal X–ray structure analysis. These gold(I) complexes show moderate potential anti–cancer activities against A549 (human lung carcinoma), HCT15 (human colon cancer), and HeLa (human cervical cancer) cell lines.

Keywords: 1,3–Bis(2,6–di–isopropylphenyl)imidazol–2–ylidenegold, dithiocarbamate gold(I) complexes, IR and NMR spectroscopic studies, *in vitro* cytotoxicity.

1. Introduction

Organometallic compounds of coinage metals (Cu, Ag and Au) have extensively been investigated owing to their diverse applications in bioinorganic and medicinal chemistry. Among coinage metals, gold complexes have attracted considerable attention in the treatment of many chronic diseases, viz. rheumatoid arthritis, bronchial asthma and cancer due to their interesting physico-chemical, biological and pharmacological properties. Both gold(I) and gold(III) complexes bearing different functional ligands have numerous bio-medical applications [1–4].

Gold(I) complexes are potential chrysotherapeutic agents, which manifest outstanding antiproliferative activity against specific human cancer cell lines that are resistant or sensitive to classical chemotherapeutic platinum drugs [4, 5]. The novelty of Au(I) based drugs is the characteristic molecular structure that allows them to overcome resistant pathways, those were encountered in platinum-based chemotherapy. In case of gold drugs, DNA is not a major pharmacological target but other enzymes related inhibitions are also involved [5].

Currently carbene complexes are significant that falls within the field of medicine. Particularly, gold carbene complexes are slowly but surely joining mainstream chemistry because of applications in the medicinal and biochemical fields [6]. The antiarthritic gold(I) phosphine compound, auranofin (AF) shows interesting antitumor *in vitro* as well as *in vivo* activity. It also inhibits glutathione S-transferase expression in several chemoresistant tumors [7]. I. Ott pointed out that N-heterocyclic carbenes, an interesting

class of ligands resemble to phosphines with donor properties [8]. Baker *et al.* reported the mononuclear, cationic, linear Au(I) N-heterocyclic carbene species inducing dose-dependent mitochondrial swelling in isolated rat liver [9] . Barnad *et al.* also described a series of (bis)NHC‑gold(I) complexes bearing the induction of mitochondrial swelling, which was directly affected by lipophilicity [10]. Siciliano *et al.* prepared Bis(1,3-dimethylimidazol-2-ylidene)gold(I) nitrate and bis(4,5-dichloro-1,3-dimethylimidazol-2-ylidene)gold(I) nitrate salts via transmetallation of their silver precursors with chloro dimethylsulfide gold and determined the anticancer properties using NCI-H460 lung cancer cells [11].

Gold complexes with dithiocarbamate ligands have also emerged as anticancer agents and have shown much promising results [12]. Ronconi *et al.* prepared and characterized some novel gold(III) dithiocarbamate compounds containing N,N–dimethyldithiocarbamate and ethyl sarcosine dithiocarbamate, demonstrating very encouraging chemical and biological profile [13]. The treatment with dibromo(N,N–dimethyldithiocarbamato)gold(III) complex resulted in significant inhibition of *in vivo* MDA–MB–231 breast tumor growth [14]. Zhang *et al.* reported gold(I)–dithiocarbamato species, namely [Au(ESDT)] could inhibit the chymotrypsin–like activity of purified 20S proteasome and 26S proteasome in human breast cancer MDA–MB–231 cells [15].

Worldwide, lung and colorectal cancers are common causes of cancer–related death in men and women while a cervical cancer is overwhelmingly major cause of cancer deaths among women [16]. Chemotherapy is still the primary method for treating cancers followed by radiotherapy. Nevertheless, there are some major challenges for treating

cancers which include intrinsic resistance, different phenotypes of cancer and systemic toxicity issues. Therefore, new chemotherapeutic modalities are required. New gold carbene complexes are being developed incorporating correct activity-enhancing and bio-acceptable co-ligands like dithiocarbamte with specific inherent properties for bio-medical applications. Based on this strategy, a novel series of gold(I) complexes may be developed with new combination of C and S donor atoms of carbene and dithiocarbamate ligands respectively that show enhanced selectivity for such resistant cancers and with fewer side–effects in comparison to platinum based drugs.

In the present work, gold(I) complexes of 1,3–Bis(2,6–di–isopropylphenyl)imidazol–2–ylidenegold (Ipr) with dialkyl/diaryl dithiocarbamate ligands as new potential chry-sotherapeutic agents were prepared. The structure determination of the prepared crystalline gold(I) complexes is carried out by single crystal X–ray diffraction. The crystallographic data is further validated by IR spectra and ^{1}H as well as ^{13}C NMR measurements. These well characterized gold(I) carbene complexes have been evaluated for *in vitro* cytotoxic activity against various human cancer cell lines e.g. A549 (human lung carcinoma), HCT15 (human colon carcinoma), and HeLa (human cervical cancer) cell lines using MTT assay.

2. Results and Discussions

2.1. Spectroscopic Characterization

Dithiocarbamate compounds exhibited characteristic band in the 1480–1550 cm^{-1} region attributed to the ν(C–N) and ν(C–S) stretching vibration [17]. The most prominent bands for complexes (**1**–**3)** were observed at 1470 cm^{-1}, 1471cm^{-1} and 1473 cm^{-1}, respectively ascribed to the thioureide band, ν(C–N). Since these frequency modes lies in between

those associated with single C–N and double C=N bonds, hence the partial double bond character of 'thioureide' bond was confirmed for all complexes [18]. The presence of the thioureide band between 1545–1430 cm^{-1}, suggested a considerable double bond character in the C…N bond vibration of the $S_2C–NR_2$ group [19]. The stretching vibration from this partial double bond is due to the partial delocalization of electron density within the dithiocarbamate [20]. The C=S thiocarbonyl stretch in complexes (**1–3)** splits into two peaks (doublet) at 1058 cm^{-1}, 979 cm^{-1}, 1062 cm^{-1}, 991 cm^{-1} and 1077 cm^{-1}, 975 cm^{-1} with medium intensity, respectively. The presence of splitting to the ν(C–S) bands in the range 975–991 cm^{-1} indicates the monodentate nature of dialkyl dithiocarbamate ligands in the synthesized complexes [21-24]. In addition to the polar thioureide ion bands $S_2C=N^+R_2$, the usual bands for sp^3 and sp^2 hybridized carbon–hydrogen stretches were observed ca. in the range 3000–2840 cm^{-1} similar to the reported sodium salt of diethyldithiocarbamate [25]. Furthermore, the stretching bands attributed to the aromatic (phenyl) and saturated aliphatic C–H methyl group of coordinated dialkyl dithiocarbamate was given in Table 1 [26-31].

The ^1H NMR chemical shifts of complexes (**1–3**) along with their corresponding metal precursor [(Ipr)Au(Cl)] and free dialkyl dithiocarbamate ligands are listed in Table 2. In all the complexes slight shifts for proton(s) of the coordinated dimethyl dithiocarbamate, diethyl dithiocarbamate and dibenzyldithiocarbamte have been observed as compared to free dialkyl dithiocarbamate ligands. The ^{13}C NMR chemical shifts of complexes (**1–3**) along with their corresponding metal precursor [(Ipr)Au(Cl)] and free dialkyl dithiocarbamate ligands are presented in Table 3. There are upfield chemical shifts of CH_3, CH_2 and C=S carbons of coordinated dialkyl dithiocarbamate with respect to free

dialkyl dithiocarbamate ligands. The ^{13}C chemical shifts of C=S carbon of dimethylthiocarbamate, dimethylthiocarbamate and dibenzyl thiocarbamate were observed in the range 206–213 ppm.

2.3. Crystal structure analysis

2.3.1. Crystal structure of complex [Au(Ipr)($S_2CN(CH_3)_2$)](1)

The molecular structure of complex [Au(Ipr)($S_2CN(CH_3)_2$)] (**1**) is shown in Figure 1. In the asymmetric unit, there are two molecules with same geometry and coordination moiety. There is a linear geometry (containing Ipr and dimethyl thiocarbamate ligand molecules) around central gold atoms in each molecule. Dimethyl thiocarbamate is acting as a coordinated counter anion in this complex molecule. The central gold(I) atom is coordinated with one C donor atom of the Ipr ligand molecule and S atom of $(S_2CNMe_2)^-$ counter anion. The Au atom adopts a most familiar linear C–Au–S coordination geometry like gold (I) complexes.

The Au–S and Au–C bond average distances are 2.30 (17) and 2.00 (6) Å respectively. The C–Au–S average bond angle 175.22 (2)°. The bond angle around Au(I) atom show considerable deviation from the ideal linear angle value 180° (Tables 4 and 5).

The Au–S bond distances are different to those found in complex [32]. Similarly, the S–Au–C bond angle is also considerably different from those found in [$Et_3PAu(S_2CNEt_2)$] complex [33] and other mononuclear $[(t\text{–}Bu)PAu]^+$ complexes [33-38] with linear geometry with gold central atom. This variation in bond angle is attributed to presence of different coordination environment in the reported complexes and this structure.

2.3.2. Crystal structure of complex [Au(Ipr)($S_2CN(C_2H_5)_2$)] (2)

There four virtually identical molecules in the asymmetric unit of x-ray structure of gold(I) complex containing the same Ipr ligand molecule and $[(S_2CNEt_2)]^-$ counter ion as shown in Figure 2. In all molecules, gold(I) is coordinated with one C donor atom of Ipr ligand molecule and one S donor atom of the $[(S_2CNEt_2)]^-$ ligand molecule.

The Au–S bond distances are almost same and around 2.31 (5) Å in all four molecules. The Au–C bond distances are also similar and around 2.00 (2) Å, which is close to double bond. The Au–S bond distances are very much similar to [Au(Ipr)($S_2CN(CH_3)_2$)] **(1)** complex and comparable with [$Et_3PAu(S_2CNEt_2)$] complex [32]. The Au–C bond distance is almost identical as found in complex **(1)**.

The geometry around Au(I)metal atom is conventionally linear and similar to each other and complex (1). In this structure S–Au–C bond angles are around 172.00 (2)°. There is a big distortion from ideal linearity in each molecule as seen in complex **(1)**. These bond angle values around central gold atom in all four molecules confirm the presence of pseudo distorted linear geometry around gold(I) atoms in this structure. These bond angle values also show big deviation from ideal linear angle of 180° (Table 5). The overall geometry of [Au(Ipr)($S_2CN(C_2H_5)_2$)] **(2)** closely resembles to those Au(I) complexes [33-38].

2.3.2. Crystal structure of complex [Au(Ipr)($S_2CN(C_7H_7)_2$)](3)

Molecular structure of [Au(Ipr)($S_2CN(C_7H_7)_2$)] **(3)** is shown in Figure 3. In this structure gold(I) is coordinated with one C donor atom and one S donor atom of two different type ligands.

The Au–Sand Au–C bond distances are 2.2999 (12) and 2.001 (5) Å respectively. The Au–C and Au–S bond distances are similar to complexes (1) and (2) and comparable with $[Et_3PAu(S_2CNEt_2)]$ complex [32]. The geometry around Au(I) metal atom is linear and similar to complexes **(1** and **2)** and other Au(I) complexes [33-36]. In $[Au(Ipr)(S_2CN(C_7H_7)_2)]$ (3) structure S–Au–C bond angle is170.76 (13)°. The bond angle value around central gold atom in this molecule confirm the presence of pseudo distorted linear geometry around gold(I) atom. This bond angle value is considerably different than complexes (**1** and **2**). This bond angle value also show big deviation from ideal linear angle of 180° (Table 5).

2.4. *In vitro* cytotoxic effects of complexes (1), (2) and (3)

The *in vitro* cytotoxicity tests were carried out for the gold(I) precursor, labeled as (**0**) and the three synthesized complexes labeled as **(1), (2)** and **(3**) and compared with cisplatin (standard classical anticancer drug) against three human cancer cell lines, HCT15, HeLa and A549 using MTT assay. The dose dependent cytotoxic effect was obtained by the stipulated increase in concentrations of cisplatin and gold complexes **(0–3)** against the fixed number of human cancer cells. The IC_{50} concentration of cisplatin and complexes **(0–3)** for different human cancer cell lines was obtained from a curve between compound concentration and percentage viability of cells (Figures 4 to 9, Table 6).

In phase contrast micrographs, a decreasing cell density and deformed cellular morphology could be observed with increasing concentration of complexes **(0–3)** (Figures 10 to 12). The dose dependent decrease in cell density was further supported by assessment of decreasing percent cell viability in MTT assay (Figures 4 to 9). The IC_{50}

189 concentrations of gold complexes were calculated from a separate curve between
190 complex concentration and %viability of cells plotted in Microsoft Excel 2007 (graphs
191 not shown) using MTT assay data and explained by logarithmic regression equations
192 (equations not shown).
193
194 All the synthesized complexes (**1**-**3**) exhibit moderate anticancer activity ranging between
195 24.5 to 180.2 μM in accordance to previous reports on anticancer studies of gold
196 complexes. These complexes showed better anti-cancer activity than free gold(I)
197 precursor, this could be attributed to dithiocarbamate ligands bonded to central gold(I)
198 ion. Our studies suggest that dithiocarbamate ligands are better leaving group than
199 chloride ion and facilitate the availability of gold atom to interact with cancer cells to
200 inhibit their growth *in vitro*. The IC_{50} values of complexes (**1**-**3**) against A549 and HeLa
201 cell lines were higher than classical anticancer drug, cisplatin. The IC_{50} values against
202 HCT15 cell line of synthesized complexes (**2** and **3**) show moderate potency but better
203 than cisplatin [37–40].

204 **3. Conclusions**

205 Gold complexes are well known for their broad spectrum of therapeutic and cytotoxic
206 activity against pathogen agents, together with their lack of cross–resistance with
207 antibiotics. The X–ray structures of all three complexes (**1**, **2** and **3**) with CAuS moiety
208 have nearly linear geometry which is typical for gold(I) complexes.
209 The high IC_{50} values against all three cancer cell lines are due to strong Au–C bond and
210 bulky carbene ligand. These factors slow down the dissociation of gold complex and its
211 interaction with cancer cells. According to our observation, this is the major factor for

slow inhibition of growth of cancer cell lines for all (**1**, **2** and **3)** complexes. The *in vitro* cytotoxicity of gold complexes (**2** and **3**) was quite promising and better than cisplatin. All the three complexes show good selectivity of inhibition of growth of HCT15 cancer line.

4. Experimental

4.1. Materials and methods

All the reactions were carried under normal ambient conditions. All chemical and solvents used in the synthesis were of analytical grade and were used without further purification. All chemicals were purchased from Sigma–Aldrich St. Louis, Missouri United States and Strem Chemicals, Massachusetts, United States.

Elemental analyses were performed on Perkin Elmer Series 11 (CHNS/O), Analyzer 2400. The solid state FTIR spectra of the ligands and their gold(I) complexes were recorded on a Perkin–Elmer FTIR 180 spectrophotometer or NICOLET 6700 FTIR using KBr pellets over the range 4000–400 cm^{-1}.

^{1}H and ^{13}CNMR spectra were recorded on a LAMBDA 500 spectrophotometer operating at 500.01, 125.65 and 200.0 MHz respectively; corresponding to a magnetic field of 11.74 T. Tetramethylsilane (TMS) was used as an internal standard for ^{1}H and ^{13}C. The ^{13}C NMR spectra were obtained with ^{1}H broadband decoupling, and the spectral conditions were: 32 k data points, 0.967 s acquisition time, and 1.00 s pulse delay and 45° pulse angle. The ^{1}H and ^{13}CNMR chemical shifts are given in Tables 2–3 respectively.

4.2. Syntheses of gold(I) complexes

4.2.1 Synthesis of [Au(Ipr)($S_2CN(CH_3)_2$)] (1)

1,3–Bis(2,6–di–isopropylphenyl)imidazol–2–ylidenegold(I)chloride, [(Ipr)Au(Cl)] (0.311 g, 0.05 mmol) in 10 mL ethanol was added drop wise to a ethanolic solution of sodium dimethyldithiocarbamate monohydrate (0.072 g,0.05 mmol) at room temperature with continuous stirring for 3h. Subsequently 1–3 mL of water was added to the reaction mixture to get the clear solution. The clear yellow solution obtained was filtered to avoid any impurity and kept undisturbed for crystallization by slow evaporation at room temperature. After five days yellow block like crystals were obtained. A well–shaped good quality crystal was chosen for X–ray diffraction analysis. Anal. Calc. for $C_{30}H_{42}AuN_3S_2$: C, 51.05; H, 6.00; N, 5.95; S, 9.07; Found: C, 51.80; H, 6.33; N, 5.87; S, 8.98. Yield: 0.314 g, (89%).

4.2.2 Synthesis of [Au(Ipr)($S_2CN(C_2H_5)_2$)] (2)

This complex was synthesized with sodium diethyldithiocarbamatetrihydrate (0.113 g, 0.05 mmol) by a procedure analogous to (**1**). After eight days colorless block like crystals were obtained. A suitable quality crystal was chosen for X–ray diffraction analysis. Anal. Calc. for $C_{32}H_{46}AuN_3S_2$: C, 52.38; H, 6.31; N, 5.72; S, 8.74; Found: C, 52.19; H, 6.37; N, 5.70; S, 8.68. Yield: 0.337 g, (92%).

4.2.3 Synthesis of [Au(Ipr)($S_2CN(C_7H_7)_2$)] (3)

This complex was synthesized with sodium diebenzyldithiocarbamatetrihydrate (0.136 g, 0.05 mmol) by a procedure adopted for (**1**). After seven days colorless block like crystals were obtained. A bright, good shaped crystal was chosen for X–ray diffraction analysis. Anal. Calc. for $C_{42}H_{54}AuN_3S_2$: C, 58.52; H, 6.31; N, 4.87; S, 7.44; Found: C, 58.19; H, 6.38; N, 4.78; S, 7.57. Yield: 0.357 g, (83%).

4.3. X–ray structure determination

For gold(I) complexes (**1**–**3)**, quality single were obtained from C_2H_5OH and H_2O solution, The intensity data were collected at 173 K on a two circle (x and u scans) [41] Stoe Image Plate Diffraction System, using Mo Kα graphite monochromated radiation. The structures were solved by direct methods, using the program SHELXS–97 [42]. The refinement and all further calculations were carried out using SHELXL–97 [42]. The H–atoms were either located from Fourier difference maps and freely refined or included in calculated positions and treated as riding atoms using SHELXL default parameters. The non–H atoms were refined anisotropically, using weighted full–matrix least–squares on F2. Empirical or multiscan absorption corrections were applied using the MULSCANABS routines in PLATON [43]. Figures 1–3 were drawn using the programs ORTEP and MERCURY [44]. A summary of crystal data and refinement details for gold(I) complexes (**1**–**3)** are given in Table 4. Selected bond lengths and bond angles are given in Table 5.

4.4. *In vitro* cytotoxic activity against A549, HCT15 and HeLa human cancer cell lines

In the present study, metal precursor and three synthesized compounds (**1**–**3)** were evaluated for their *in–vitro* cytotoxic activity against HCT15 (human cancer), HeLa (human cervical cancer) and A549 (human lung carcinoma) cell lines. The cells were seeded at 4 x 10^3 cells/well in 100µL DMEM (Dulbecco's Modified Eagle's Medium) containing 10%. FBS (Fetal Bovine Serum) in 96–wells tissue culture plate and incubated for 72 h at 37 ^oC, 5% CO_2 in air and 90% relative humidity in CO_2 incubator. After incubation, 100 µL of complex (**0**), (**1**), (**2**) and (**3**) complexes (50, 25, 12.5 and 6.25 µg/mL), prepared in DMEM, was added to cells and the cultures were incubated for 24 h.

The medium of wells was discarded and 100 µL DMEM containing MTT (3–(4,5–Dimethylthiazol–2–Yl)–2,5–Diphenyltetrazolium Bromide) (5 mg/mL) was added to the wells and incubated in CO_2 incubator at 37 ^{o}C in dark for 4 h. After incubation, a purple colored formazan (artificial chromogenic dye, product of the reduction of water insoluble tetrazolium salts e.g., MMT by dehydrogenases and reductases) in the cells is produced and appeared as dark crystals in the bottom of the wells. The medium of culture was discarded from each well carefully to avoid disruption of monolayer and 100 µL of Dimethylsulphoxide (DMSO) was added in each well. The solution was thoroughly mixed in the wells to dissolve the formazan crystals which ultimately result into a purple solution. The absorbance of the 96–wells plate was taken at 570 nm with LabsystemsMultiskan EX–Enzyme–linked immunosorbent assay (EX–ELISA) reader against a reagent blank.

Supplementary material

Supplementary crystallographic data of CCDC deposit number are 986121, 986122 and 986123 for the complexes (**1**–**3)** respectively and can be obtained free of charge via www.ccdc.cam.ac.uk/data_request/cif, by e–mailing data_request@ccdc.cam.ac.uk, or by contacting the Cambridge Crystallographic Data Centre, 12 Union Road, Cambridge CB2 1EZ, UK; fax: +44(0)1223–336033.

Acknowledgement

The author(s) would like to acknowledge the support provided by King Abdulaziz City for Science and Technology (KACST) through the Science & Technology Unit at King

Fahd University of Petroleum & Minerals (KFUPM) for funding this work through project No. **11–MED1670–04** as part of the National Science, Technology and Innovation Plan.

References

[1] K. Nomiya, R.S. Yamamoto, Noghuchi, H. Yokoyama, N.C. Kasuga, K, Ohyama, C. Kato, J. Inorg. Biochem. 95 (2003) 208–220.

[2] T. McCormick, W.–L.Jia, S. Wang, Inorg. Chem. 45 (2006) 147–155.

[3] S.S. Al–Jaroudi, M.I.M. Wazeer, A.A. Isab, S. Altuwaijri, Polyhedron (2013) 434–442.

[4] R. B. Bostancioglu, K. Isik, H. Genc, K. Benkli, A.T. Koparal, Medicinal Chemistry. 27 (2012) 458–466.

[5] S. H. van Rijt, P.J. Sadler, Drug Discovery Today, 14 (2009) 1089–1097.

[6] H. G. Raubenheimer, S. Cronje, Chem. Soc. Rev., 37 (2008) 1998-2011.

[7] R. Noghuchi, A. Hara, A. Sugie, K. Nomiya, Inorg. Chem. Commun. 9 (2006) 355–359

[8] I. Ott, Coordination Chemistry Reviews, 253 (2009) 1670-1681

[9] M.V. Baker, P.J. Barnard, S.J. Berners-Price, S.K. Brayshaw, J. L.Hickey, B.W. Skelton, A.H. White, Dalton Trans., 30 (2006) 3708-3715.

[10] P.J. Barnard, S.J. Berners-Price, Coord. Chem. Rev., 251 (2007) 1889‑1902.

[11] T. J. Siciliano, M. C. Deblock, K.M. Hindi,S. Durmus, M. J. Panzner, C. A. Tessier, W. J. Youngs, Journal of Organometallic Chemistry**, 696** (2011) 1066-1071.

[12] G. Boscutti , L. Feltrin , D. Lorenzon , S. Sitran , D. Aldinucci , L. Ronconi and D. Fregona, Inorg. Chim. Acta, 393 (2012) 304-317.

[13] L. Ronconi, L. Giovagnini, C. Marzano, F. Bettio, R. Graziani, G. Pilloni, D. Fregona, Inorg. Chem. 44 (2005) 1867–1881

[14] V. Milacic, D. Chen, L. Ronconi, K. R. Landis–Piwowar,D. Fregona, Q. P. Dou,Cancer Res. 66(2006)10478–10486.

[15] X. Zhang, M. Frezza, V. Milacic, L. Ronconi, Y. Fan, C. Bi, D. Fregona, Q. P. Dou, J. Cell Biochem. 109 (2010) 162–172.

[16] K. Nomiya, R. Noghuchi, K. Ohsawa, K. Tsuda, M. Oda, J. Inorg. Biochem. 78 (2000) 363–370.

[17] A. J. Odola, J. A. O. Woods, J. Chem. Pharm. Res., 3 (2011) 865–871.

[18] F. Jian, Z. Wang, Z. Bai, X. You, H. Fun, K. Chinnakali, L.A. Razak, Polyhedron, 18 (1999) 3401–3406.

[19] A. Jayaraju, M. M. Ahamad, R. M. Rao, J. Sreeramulu, Der PharmaChemica, 4 (2012) 1191–1194.

[20] H. Nabipour, S. Ghammamy, S. Ashuri, Z. S. Aghbolagh, J. Org. Chem., 2 (2010) 75–80.

[21] J. Chatt, L. A. Duncanson, L. M. Venanzi, Nature, 177 (1956)1042–1043.

[22] I. Raya, I. Baba, B. M. Yamin, Malaysia Journal of Analytical Sciences, 10 (2006) 93–98.

348 [23] W. Haas, T. Schwarz, Microchem. Ichonal.Acta, 58 (1963) 253–259

349 [24] D.C. Onwudiwe, P.A. Ajibade, Polyhedron, 29 (2010) 1431–1436

350 [25] C. J. Pouchert, Aldrich Library of FT–IR Spectra, 2nd ed.; Aldrich Chemical
351 Company: Milwaukee, Vol. 1 (1997).

352 [26] D. L. Pavia, G. M. Lampman, S. G. Kriz, Introduction to Spectrochemistry. 3rd
353 Ed., Thomson Learning, USA., (2001) 30–33.

354 [27] R. M. Silverstein, F. X. Webster, Spectrometric Identification of Organic
355 Compounds, 6th edition (Wiley, New York, 1998) and T. W. G. Solomons, C.
356 Fryhle Organic Chemistry, 7th edition upgrade (Wiley, New York, 2001).

357 [28] K. N. Kouroulis, S. K. Hadjikakou,N. Kourkoumelis,M. Kubicki,L. Male,M.
358 Hursthouse,S. Skoulika,A. K. Metsios, V. Y. Tyurin,A. V. Dolganov,E. R.
359 Milaevag, N. Hadjiliadis, J. Chem. Soc. Dalton Trans, (2009) 10446–10456.

360 [29] E. A. Allen, W. Wilkinson, Spectrochim. Acta, 2 (1972) 2257–2262.

361 [30] I. S. Butler, A. Neppel, K. R. Plowman, C. F. Shaw, J. Raman Spectrosc., 15
362 (1984) 310–318.

363 [31] A. G. Jones, D. B. Powell, Spectrochim. Acta, 30 (1984) 563–570.

364 [32] S.Y. Ho, E.R.T. Tiekink, Z. Kristallogr. 220 (2005) 342–344.

365 [33] I. Sänger, H.–W. Lerner, T. Sinke, M. Bolte, Acta Cryst. E68 (2012) m708.

366 [34] P. Lu, T. C. Boorman, A.M.Z. Slawin, I. Larrosa, J. Am. Chem. Soc.132 (2010)
367 5580–5581.

368 [35] R. E. Marsh, Acta Cryst. B58 (2002) 893–899.

369 [36] H. Schmidbaur, B. Brachthiuser, O. Steigelmann, H. Beruda, Chem. Ber. 125
370 (1992) 2705–2710.

[37] E. Barreiro, J.S. Casas, M.D. Couce, A. Sánchez, J. Sordo, E.M. Vázquez–López, J. Inorg. Biochem.131 (2014) 68–75.

[38] R. Kivekäs, E. Colacio, J. Ruiz, J.D. López–González, P. León, Inorg. Chim.Acta. 159 (1989) 103–110.

[39] L. Ortego, F. Cardoso, S. Martins, M.F. Fillat, A. Laguna, M. Meireles, M.D. Villacampa, M.C. Gimeno, J. Inorg. Biochem.130 (2014) 32–37.

[40] I. Ott, T. Koch, H. Shorafa, Z. Bai, D. Poeckel, D. Steinhilber, R. Gust,Org. Biomol. Chem. 3 (2005) 2282–2286.

[41] Stoe, Cie, X–Area V1.35 and X–RED32 V1.31 Software, Stoe and Cie GmbH, Darmstadt, Germany, 2006.

[42] G.M. Sheldrick, ActaCryst. A64 (2008) 112–122.

[43] A.L. Spek, ActaCryst. D65 (2009) 148–155.

[44] C.F. Macrae, P.R. Edgington, P. McCabe, E. Pidcock, G.P. Shields, R. Taylor, M. Towler, J. van de Streek, J. Appl. Crystallogr. 39 (2006) 453–457.

Complex (**0**)

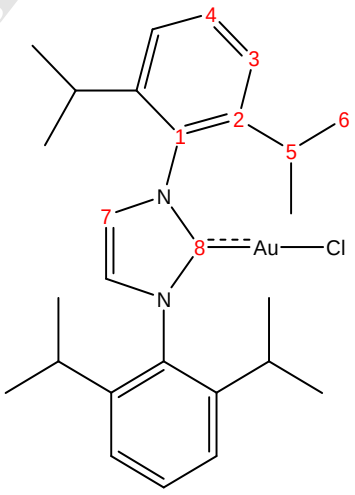

388 [(Ipr)Au(Cl)]

389

390 Complex (**1**)

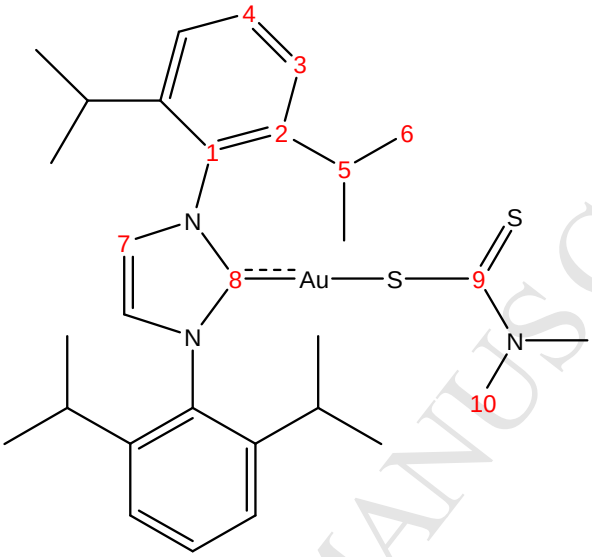

391

392 [(Ipr)Au($S_2CN(CH_3)_2$)]

393

394

395 Complex (**2**)

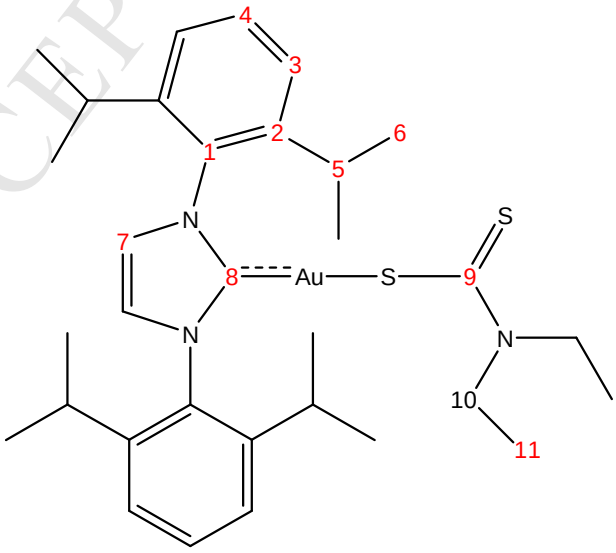

396

[(Ipr)Au($S_2CN(C_2H_5)_2$)]

Complex (**3**)

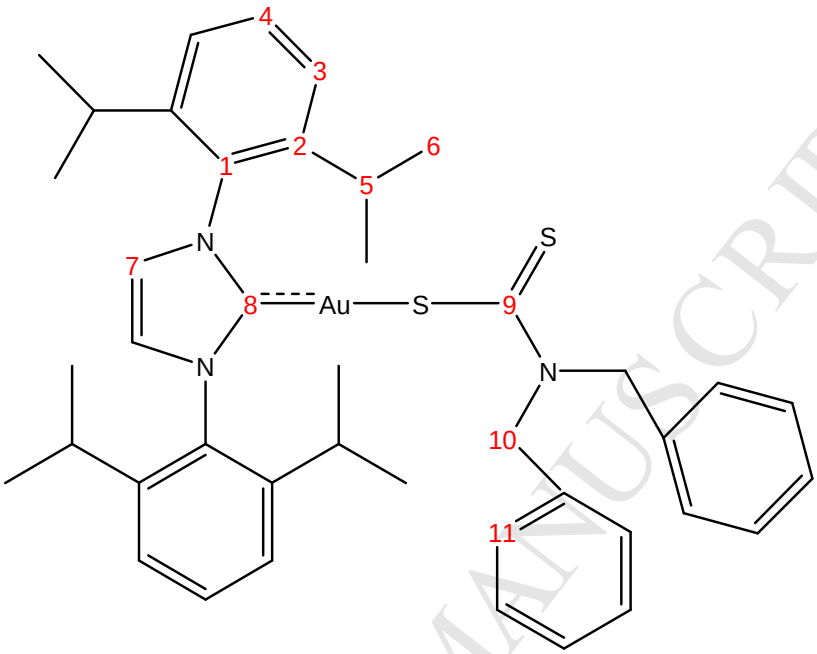

[(Ipr)Au($S_2CN(C_7H_7)_2$)]

Scheme 1: Skeletal structures and condensed formulae of complexes (**0), (1), (2)** and **(3)** representing non–equivalent carbons and protons for ^{1}H and ^{13}C NMR data.

Table 1: Mid–IR frequencies (cm^{-1}) of complexes **(1–3)**

Compound	Stretch	Bend	Stretch	Bend	Stretch	Stretch
	C–H(CH_3)	C–H(CH_3)	C–H(CH_2)	C–H(CH_2)	C=S	S=C–N
Dimethyl dithiocarbamate	2924	1360	——	——	962	1488
(**1**)	2961(asym), 2866 (sym)	1361	——	——	1058, 979	1470
Diethyl dithiocarbamate	2925	1358	2979	1379	986	1466
(**2**)	2962(asym), 2867 (sym)	1377	2926	1407	1062, 991	1473
Dibenzyl dithiocarbamate	2960(asym), 2868 (sym)	1347	——	1445	1075, 987	1491
(**3**)	2961(asym), 2865 (sym)	1395	2923	1451	1077, 975	1471

406

407

408 Table 2: Solution ^{1}H NMR δ chemical shifts (ppm) and ^{n}J couplimg constants (Hz) of
409 the free gold(I) metal precursor, free ligands and complexes **(1–3)**.

Compound	3-H ppm	$^{3}J_{CH=CH}$ Hz	4-H Ppm	$^{3}J_{CH-CH}$ Hz	5-H ppm	$^{3}J_{CH3-CH-CH3}$ Hz	6-H´ ppm	$^{3}J_{CH3-CH}$ Hz	6-H ppm	$^{3}J_{CH3-CH}$ Hz	7-H ppm	10-H Ppm	11-H ppm	^{2} Hz
[Au(Ipr)(Cl)]	7.39		7.55		2.46				1.21		7.98	–	–	
$NaS_2CN(CH_3)_2{\cdot}H_2O$	–		–		–				–		–	3.55	–	
(**1**)	7.34	7.63	7.5	7.63	2.52	7.02	1.16	7.02	1.25	6.71	7.91	3.12	–	–
$NaS_2CN(C_2H_5)_2{\cdot}3H_2O$	–		–		–				–		–	4.03	1.23	
(**2**)	7.38	7.93	7.5	7..78	2.52	7.01	1.17	7.02	1.26	6.71	7.88	3.53	1	6.87
$NaS_2CN(C_7H_7)_2{\cdot}xH_2O$	–		–		–				–		–	4.98	7.01	
(**3**)	7.33	7.93	7.5	7.63	2.53	7.02	1.15	6.71	1.26	6.71	7.91	4.85	7.11	7.63

410

411 Table 3: Solution ^{13}C NMR chemical shifts (ppm) of the free gold(I) metal precursor and
412 Au(I) complexes **(1), (2), and (3).**

Complex	C=S	Au=C	C–1	C–2	C–3	C–4	C–5	C–6	C–7	C–10	C–11
[Au(Ipr)(Cl)]	–	172.86	134.06	145.32	124.55	124.09	28.37	23.5	130.52		
$NaS_2CN(CH_3)_2{\cdot}H_2O$	212.82	–	–	–	–	–	–	–	–	45.12	–
(1)	205.66	181.9	134.5	145.34	124.33	123.85	28.34	23.84	130.13	44.31	–
$NaS_2CN(C_2H_5)_2{\cdot}3H_2O$	206.7	–	–	–	–	–	–	–	–	49.61	12.31
(2)	204.31	182.13	134.53	145.34	124.36	123.86	28.35	23.96	130.16	48	12.15
$NaS_2CN(C_7H_7)_2{\cdot}H_2O$	213.53	–	–	–	–	–	–	–	–	56.9	127–137
(3)	208.28	181.61	134.52	145.35	124.45	123.9	28.39	23.89	130.17	55.37	127–136

413

414

415

416

417

Table 4: Crystallographic characteristics, experimental and structure refinement details for crystal structure of complex complexes **(1–3)**

Parameters	Complex **1**	Complex **2**	Complex **3**
Empirical formula	$C_{30}H_{42}AuN_3S_2$	$C_{32}H_{46}AuN_3S_2$	$C_{42}H_{50}AuN_3S_2$
Empirical formula weight	705.75	733.8	857.94
Crystal size/mm	0.45×0.30×0.20	0.45×0.38×0.30	0.45 × 0.42 × 0.35
Wavelength/Å	0.71073	0.71073	0.71073
Temperature/K	173	173	173
Crystal symmetry	Monoclinic	Orthorhombic	Orthorhombic
Space group	$P2_1/c$	$Pna2_1$	$Pna2_1$
a/Å	13.2323 (4)	42.4867 (11)	25.7815 (9)
b/Å	28.9995 (11)	16.4047 (5)	12.4955 (4)
c/Å	17.1760 (5)	19.1873 (5)	12.0577 (5)
β/°	104.687 (2)°		
V/ Å^3	6375.6 (4)	4416.3 (5)	3884.4 (2)
Z	8	16	4
D_c/Mg m^{-3}	1.471	1.458	1.467
μ(Mo–Kα)/mm^{-1}	4.77	4.55	3.93
F(000)	2832	5920	1736
θ Limits/°	1.4–26.1	1.2–26.2	1.6–26.1

Collected reflections	83383	98752	25927
Unique reflections	8469	15664	6167
Observed reflections	11547	23566	7312
Goodness of fit on F^2	1	0.94	1
$R_1[F^2 > 2\sigma(F^2)]$	0.048	0.052	0.029
w$R_2(F^2)$	0.081	0.095	0.06
Largest diff. peak, hole/e Å^{-3}	3.19, −0.96	1.07, −1.30	1.24, −2.05

443

444

445
446

Table 5: Selected bond distances (Å) and bond angles (°) for complexes **(1-3).**

Complex **1**		Complex **2**		Complex **3**	
Bond Length (Å)		Bond Length (Å)		Bond Length (Å)	
Au1—S1	2.3062 (17)	Au1—C6	2.02 (2)	Au1—C16	2.001 (5)
Au2—S3	2.2985 (17)	Au1—S1	2.314 (5)	Au1—S1	2.2999 (12)
Au1—C4	2.011 (7)	Au2—C38	1.984 (17)		
Au2—C34	1.998 (6)	Au2—S3	2.301 (5)		
		Au3—C70	1.994 (19)		
		Au3—S5	2.310 (5)		
		Au4—C102	2.05 (2)		
		Au4—S7	2.307 (5)		
Bond Angles (°)		Bond Angles (°)		Bond Angles (°)	
C4—Au1—S1	175.38 (19)	C6—Au1—S	1171.2 (5)	C16—Au1—S1	170.76 (13)
C1—S1—Au1	99.7 (2)	C1—S1—Au1	101.0 (7)	C1—S1—Au1	105.3 (2)
C34—Au2—S3	175.07 (19)	C38—Au2—S3	173.7 (6)		
C31—S3—Au2	103.3 (2)	C33—S3—Au2	103.1 (7)		
		C70—Au3—S5	173.9 (6)		
		C65—S5—Au3	103.0 (6)		
		C102—Au4—S7	172.2 (5)		
		C97—S7—Au4	104.7 (7)		

456 Table 6: IC_{50} Values (μM) of gold(I) complexes against A549, HeLa and HCT15 cancer
457 cell lines.

Complex	A549	HeLa	HCT15
Cisplatin	41.6	19.4	29.5
(**0**)	180.2	172.5	121.7
(**1**)	133.9	108.3	41.1
(**2**)	91.7	79.6	24.5
(**3**)	139.9	124.6	27.4

458

459

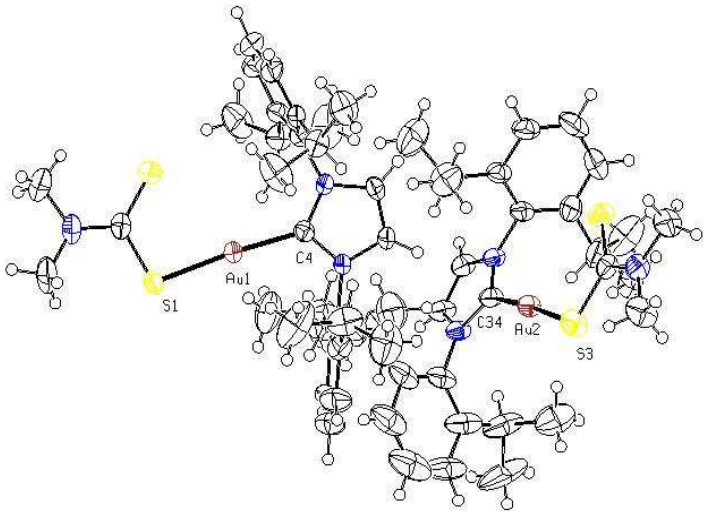

Figure 1. A view of the molecular structure of mononuclear complex (**1**), with atom labeling scheme and displacement ellipsoids drawn at 50% probability level.

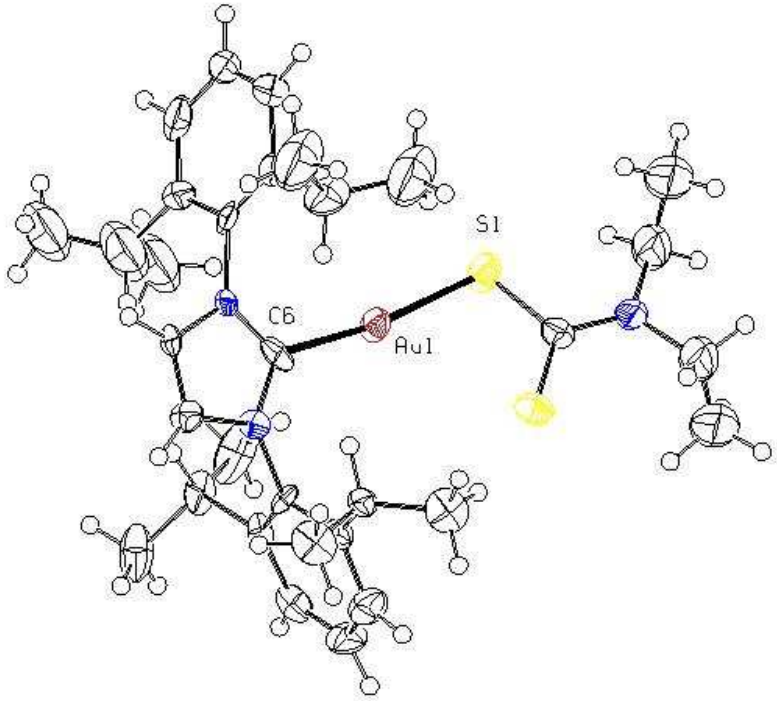

Figure 2. A view of the molecular structure of mononuclear complex (**2)**, with atom labeling scheme and displacement ellipsoids drawn at 50% probability level (Three molecules have been omitted for clarity).

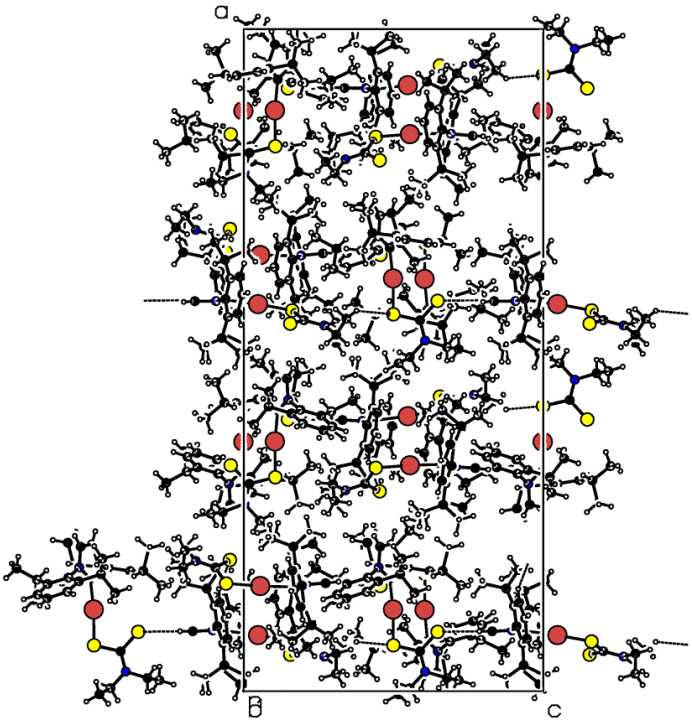

Figure 2.1. Packing diagram along *b* axis of compound (**2**), showing Hydrogen bonding network.

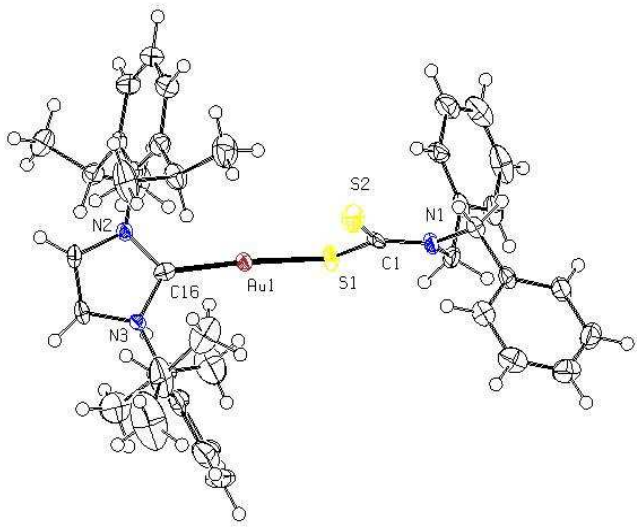

Figure 3.A view of the molecular structure of mononuclear complex (**3)**, with atom labeling scheme and displacement ellipsoids drawn at 50% probability level.

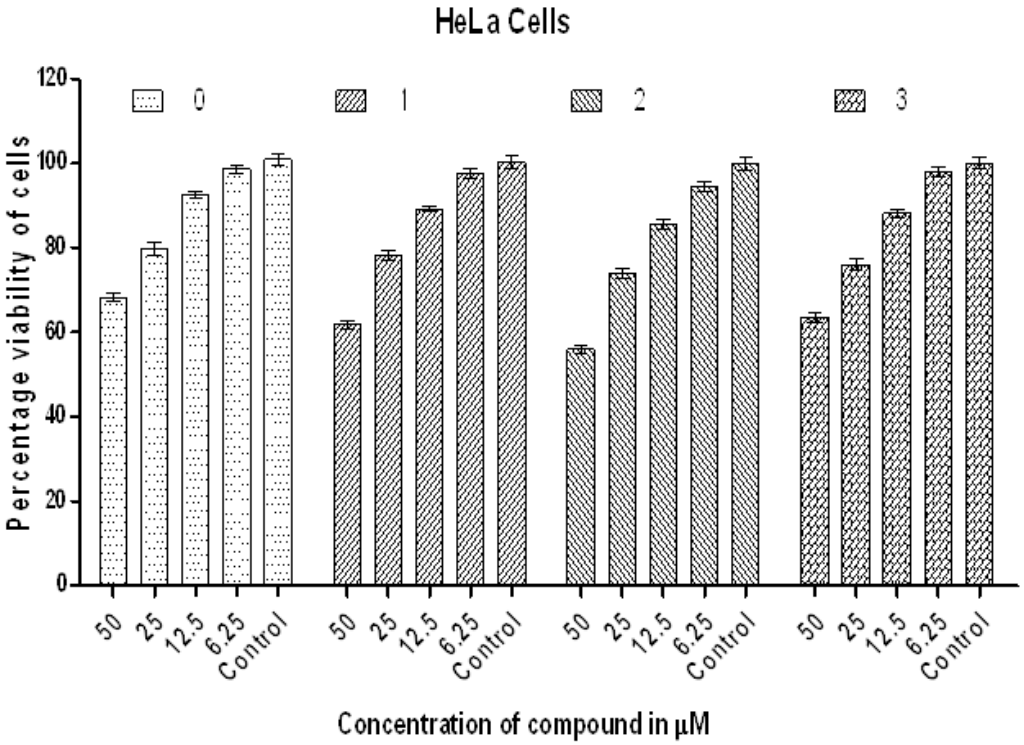

500

501 **Fig 4.** Graph showing the cytotoxic effect of series of concentrations of compounds (**0–3)**
502 on viability of HeLa cells.

503

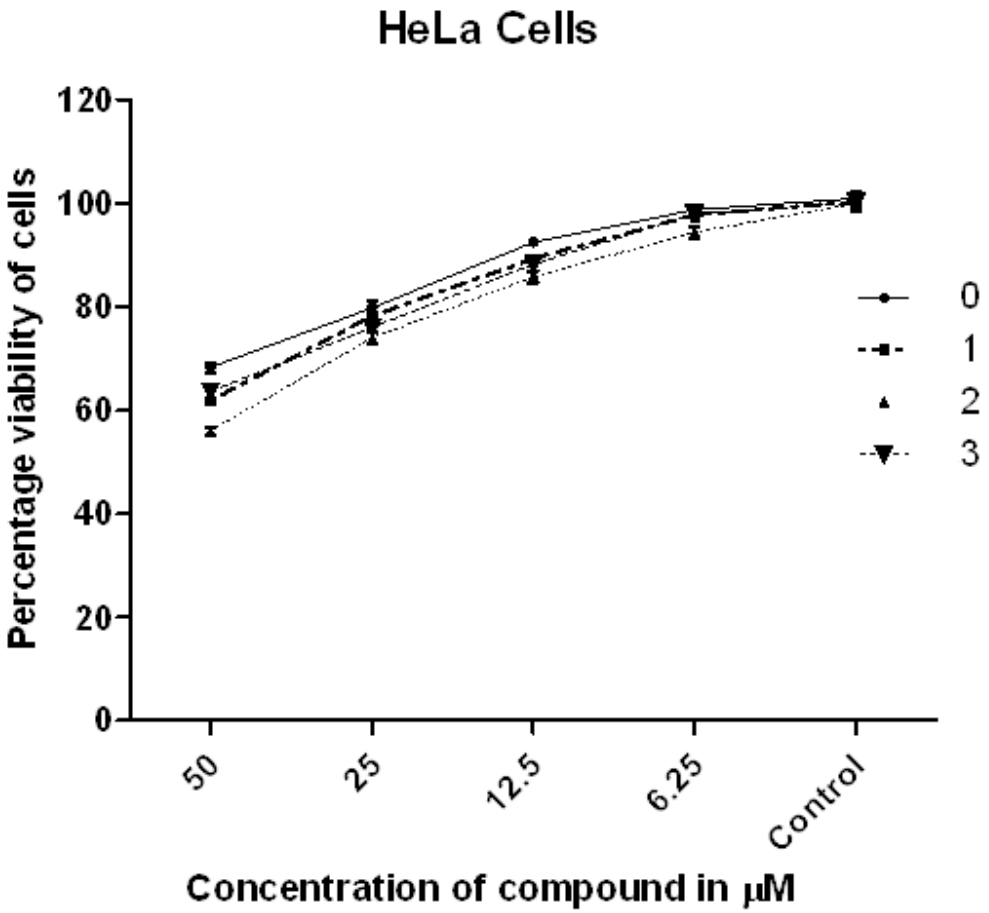

504

505 **Fig 5.** *In vitro* cytotoxic effect of series of concentrations of compounds (**0–3)** on HeLa
506 cell line.

507

508

509

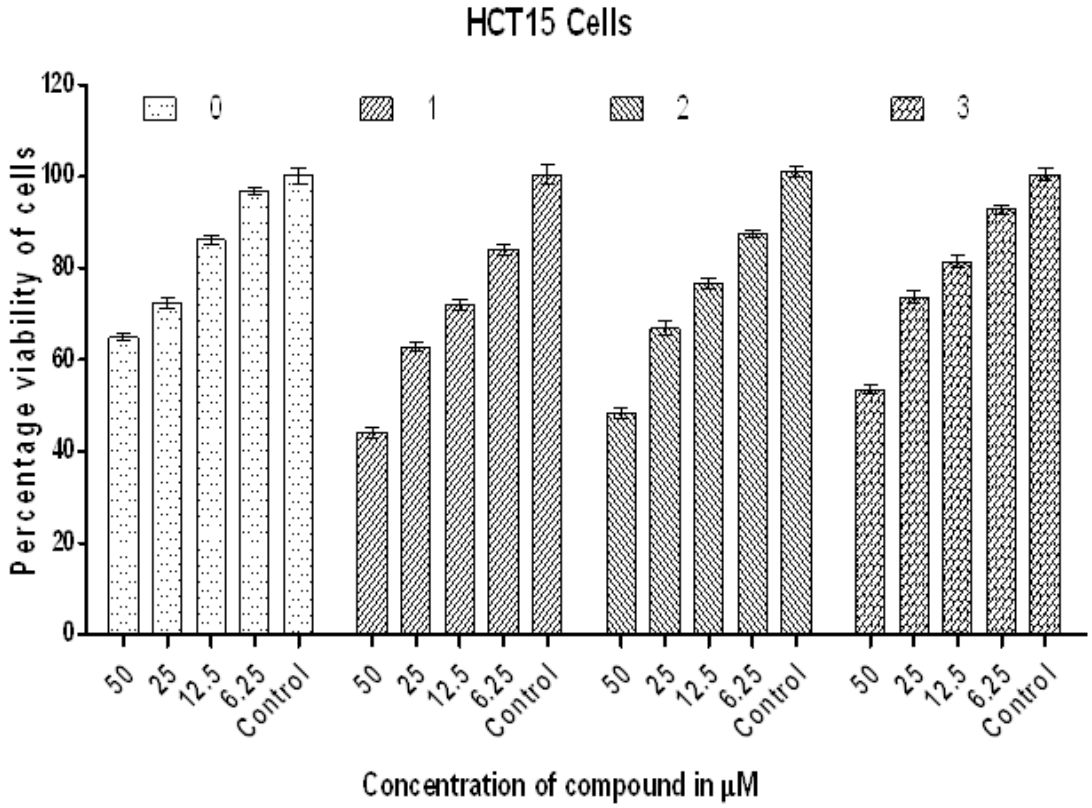

510

511 **Fig 6.** Graph showing the cytotoxic effect of series of concentrations of complex (**0–3)** on
512 viability of HCT15 cells.

513

514

515

516

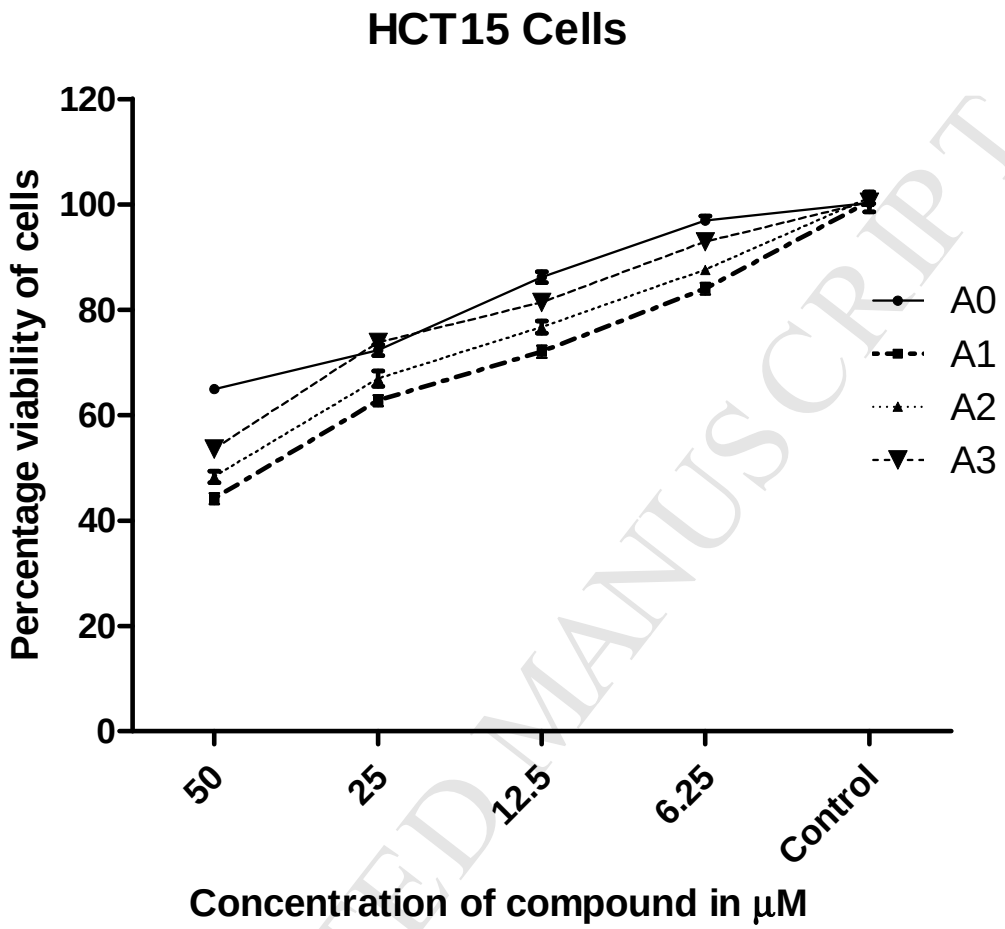

517

518 **Fig 7.** *In vitro* cytotoxic effect of series of concentrations of compounds (**0–3)** on HCT15
519 cell line.

520

521

522

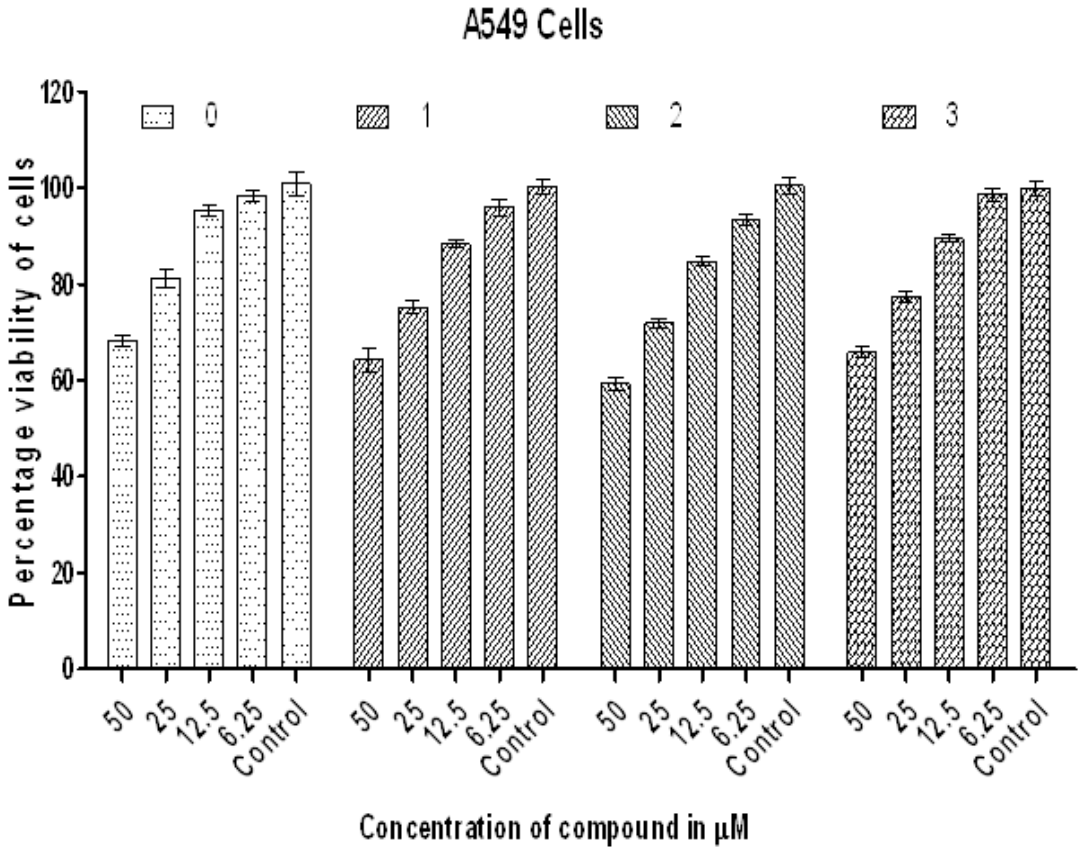

Fig 8. Graph showing the cytotoxic effect of series of concentrations of compounds (**0–3)** on viability of A549 cells.

529

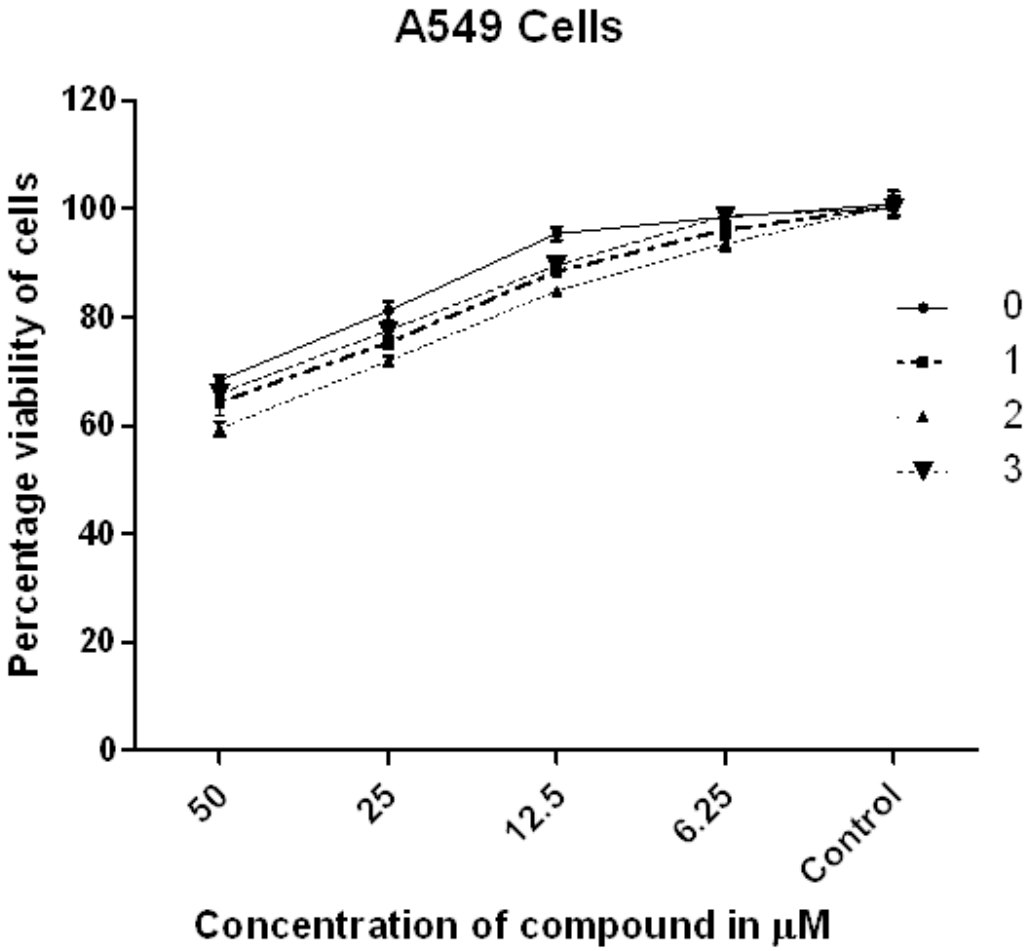

530

531 **Fig 9.** *In vitro* cytotoxic effect of series of concentrations of compounds (**0–3)** on A549
532 cell line.

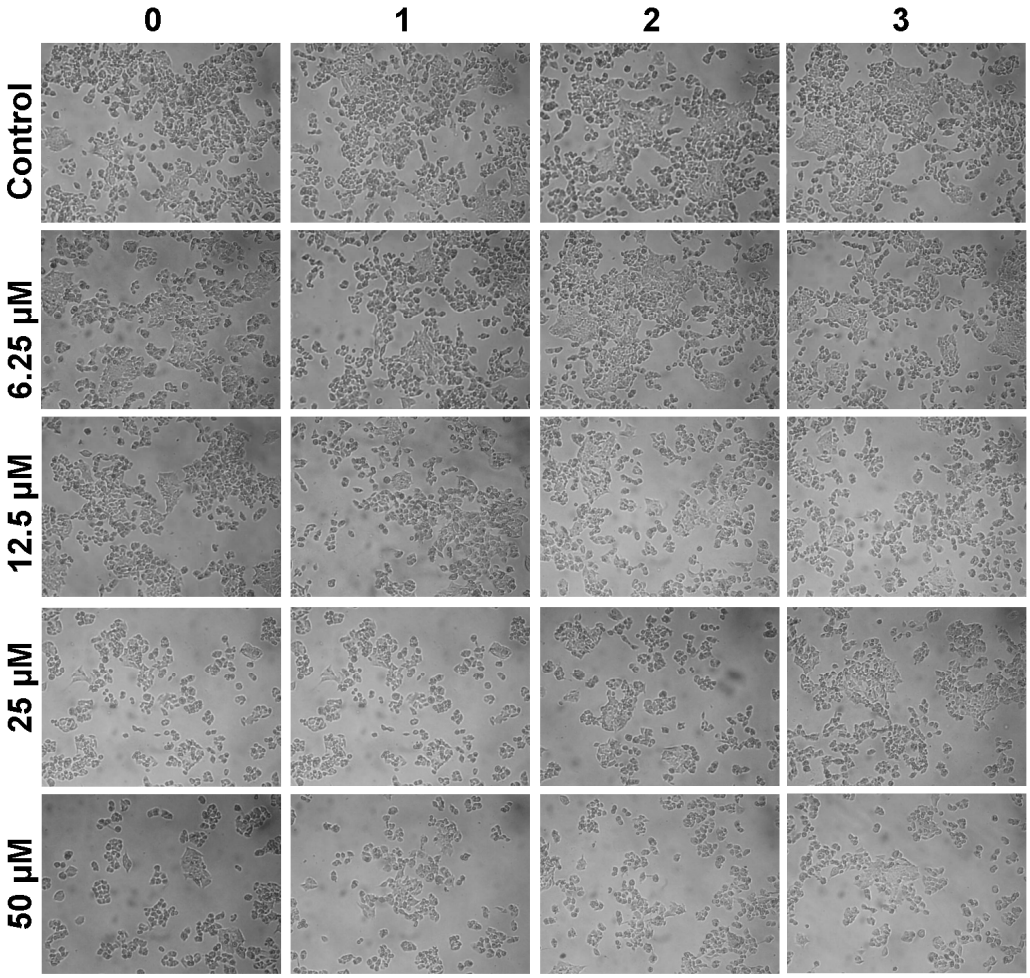

533

534 **Fig 10.** Morphological changes in HCT15 cells treated with series of concentrations of
535 compounds (0–3) studied using phase contrast microscopy.

536

537

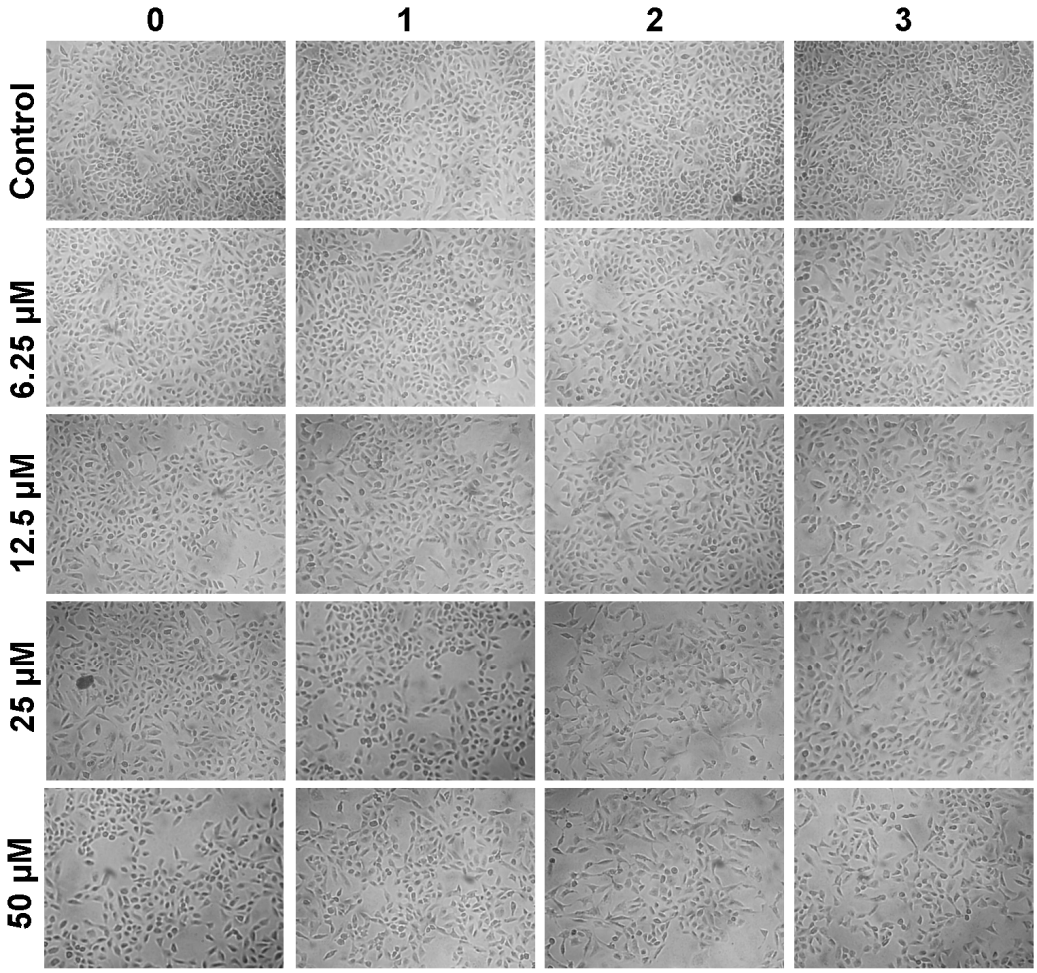

538

539 **Fig 11.** Morphological changes in A549 cells treated with series of concentrations of
540 compounds (0–3) studied using phase contrast microscopy.

541

542

543

544

545

546

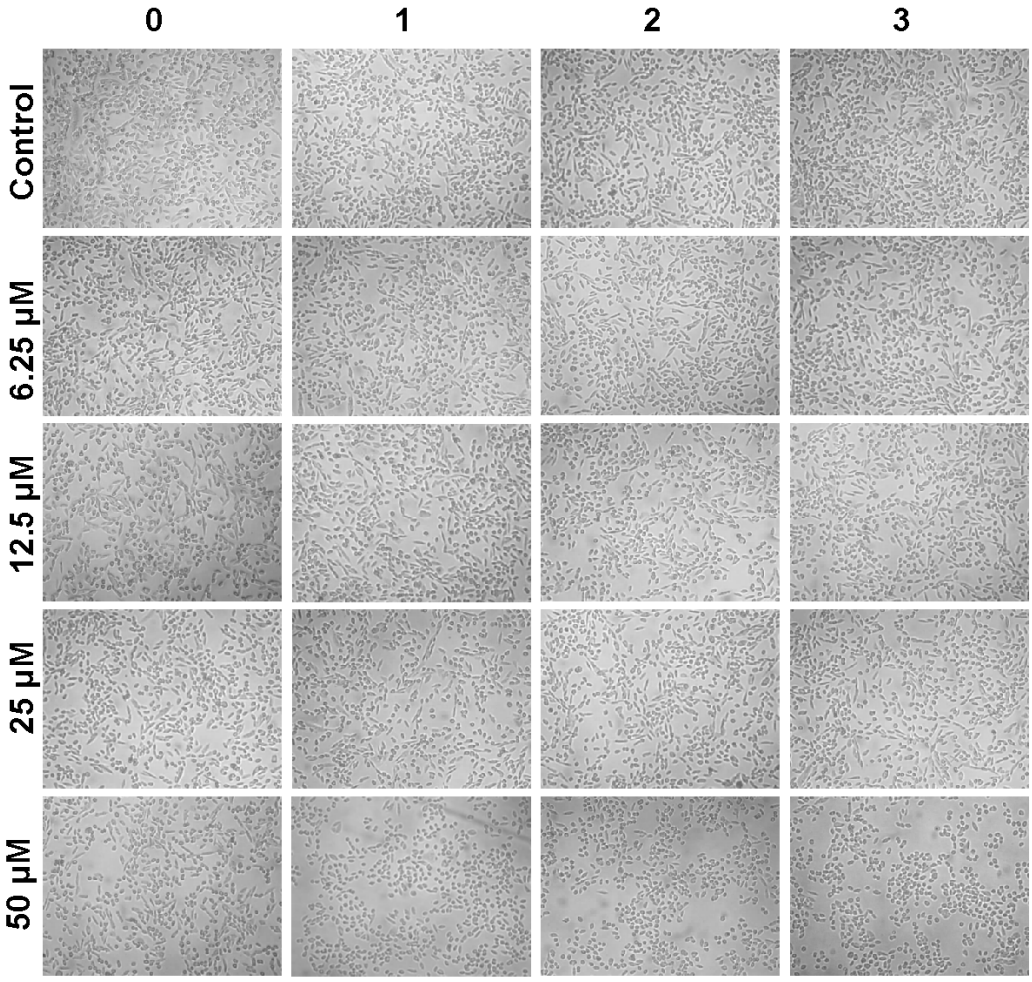

547

548 **Fig 12.** Morphological changes in HeLa cells treated with series of concentrations of
549 compounds (0–3) studied using phase contrast microscopy.

- *In vitro* studies of a new gold(I) carbene complex have been reported here.
- These complexes have been characterized by elemental analysis, IR spectroscopy and NMR measurements.
- The crystal structures of new [Au(Ipr)($S_2CN(CH_3)_2$)] (**1**), [Au(Ipr)($S_2CN(C_2H_5)_2$)] (**2**) and [Au(Ipr)($S_2CN(C_7H_7)_2$)] (**3**) [where Ipr = 1,3-Bis(2,6-di-isopropylphenyl)imidazol-2-ylidenegold] have been reported.